

LASER SHOCK PEENED COMPRESSIVE RESIDUAL
PROFILE AFTER EXPOSURE TO TEMPERATURE



CHRIS LYKINS
PAUL PREVEY
PERRY MASON

AEROPROPULSION AND POWER DIRECTORATE
WRIGHT LABORATORY
AIR FORCE MATERIEL COMMAND
WRIGHT PATTERSON AFB OH 45433-7251

SEPTEMBER 1995

FINAL REPORT FOR 01/01/94 - 06/01/94

APPROVED FOR PUBLIC RELEASE; DISTRIBUTION UNLIMITED

AEROPROPULSION AND POWER DIRECTORATE
WRIGHT LABORATORY
AIR FORCE MATERIEL COMMAND
WRIGHT PATTERSON AFB OH 45433-7251

19960325 096

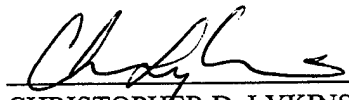
19960325 096

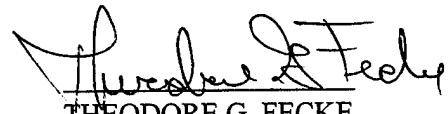
NOTICE

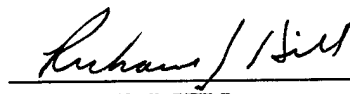
WHEN GOVERNMENT DRAWINGS, SPECIFICATIONS, OR OTHER DATA ARE USED FOR ANY PURPOSE OTHER THAN IN CONNECTION WITH A DEFINITELY GOVERNMENT-RELATED PROCUREMENT, THE UNITED STATES GOVERNMENT INCURS NO RESPONSIBILITY OR ANY OBLIGATION WHATSOEVER. THE FACT THAT THE GOVERNMENT MAY HAVE FORMULATED OR IN ANY WAY SUPPLIED THE SAID DRAWINGS, SPECIFICATIONS, OR OTHER DATA, IS NOT TO BE REGARDED BY IMPLICATION, OR OTHERWISE IN ANY MANNER CONSTRUED, AS LICENSING THE HOLDER, OR ANY OTHER PERSON OR CORPORATION; OR AS CONVEYING ANY RIGHTS OR PERMISSION TO MANUFACTURE, USE, OR SELL ANY PATENTED INVENTION THAT MAY IN ANY WAY BE RELATED THERETO.

THIS REPORT IS RELEASABLE TO THE NATIONAL TECHNICAL INFORMATION SERVICE (NTIS). AT NTIS, IT WILL BE AVAILABLE TO THE GENERAL PUBLIC, INCLUDING FOREIGN NATIONS.

THIS TECHNICAL REPORT HAS BEEN REVIEWED AND APPROVED FOR PUBLICATION.


CHRISTOPHER D. LYKINS
Project Engineer
Components Branch
Turbine Engine Division
Aero Propulsion & Power Directorate


THEODORE G. FECKE
CHIEF, Components Branch
Turbine Engine Division
Aero Propulsion & Power Directorate


RICHARD J. HILL
Chief of Technology
Turbine Engine Division
Aero Propulsion & Power Directorate

IF YOUR ADDRESS HAS CHANGED, IF YOU WISH TO BE REMOVED FROM OUR MAILING LIST, OR IF THE ADDRESSEE IS NO LONGER EMPLOYED BY YOUR ORGANIZATION PLEASE NOTIFY WL/POTC, WRIGHT-PATTERSON AFB, OH 45433-7251 TO HELP MAINTAIN A CURRENT MAILING LIST.

COPIES OF THIS REPORT SHOULD NOT BE RETURNED UNLESS RETURN IS REQUIRED BY SECURITY CONSIDERATIONS, CONTRACTUAL OBLIGATIONS, OR NOTICE ON A SPECIFIC DOCUMENT.

REPORT DOCUMENTATION PAGE			Form Approved OMB No. 0704-0188	
Public reporting burden for this collection of information is estimated to average 1 hour per response, including the time for reviewing instructions, searching existing data sources, gathering and maintaining the data needed, and completing and reviewing the collection of information. Send comments regarding this burden estimate or any other aspect of this collection of information, including suggestions for reducing this burden, to Washington Headquarters Services, Directorate for Information Operations and Reports, 1215 Jefferson Davis Highway, Suite 1204, Arlington, VA 22202-4302, and to the Office of Management and Budget, Paperwork Reduction Project (0704-0188), Washington, DC 20503.				
1. AGENCY USE ONLY (Leave blank)	2. REPORT DATE SEP 1995	3. REPORT TYPE AND DATES COVERED FINAL 01/01/94--06/01/94		
4. TITLE AND SUBTITLE LASER SHOCK PEENED COMPRESSIVE RESIDUAL PROFILE AFTER EXPOSURE TO TEMPERATURE		5. FUNDING NUMBERS C PE PR 3066 TA 12 WU TP		
6. AUTHOR(S) CHRIS LYKINS, PAUL PREVEY AND PERRY MASON				
7. PERFORMING ORGANIZATION NAME(S) AND ADDRESS(ES) AEROPROPULSION AND POWER DIRECTORATE WRIGHT LABORATORY AIR FORCE MATERIEL COMMAND WRIGHT PATTERSON AFB OH 45433-7251		8. PERFORMING ORGANIZATION REPORT NUMBER		
9. SPONSORING / MONITORING AGENCY NAME(S) AND ADDRESS(ES) AEROPROPULSION AND POWER DIRECTORATE WRIGHT LABORATORY AIR FORCE MATERIEL COMMAND WRIGHT PATTERSON AFB OH 45433-7251		10. SPONSORING / MONITORING AGENCY REPORT NUMBER WL-TR-95-2108		
11. SUPPLEMENTARY NOTES				
12a. DISTRIBUTION / AVAILABILITY STATEMENT APPROVED FOR PUBLIC RELEASE; DISTRIBUTION IS UNLIMITED.		12b. DISTRIBUTION CODE		
13. ABSTRACT (Maximum 200 words) The surface of any component that undergoes mechanical loading is particularly important in influencing the fatigue life of that part. The factors that contribute to surface fatigue sensitivity are less slip restriction at the surface, the existence of single edge cracks, the surface sees large tensile gradients when the part is exposed to bending and torsion, the surface tends to be an area of multiple defects and the surface is the most sensitive region to environmental effects such as corrosion. Compressive residual stresses are utilized in the turbine engine environment to counteract regions on the surface that must withstand high tensile stresses.				
14. SUBJECT TERMS			15. NUMBER OF PAGES 18	
			16. PRICE CODE	
17. SECURITY CLASSIFICATION OF REPORT U	18. SECURITY CLASSIFICATION OF THIS PAGE U	19. SECURITY CLASSIFICATION OF ABSTRACT U	20. LIMITATION OF ABSTRACT	

Blank Pages

TABLE OF CONTENTS

SECTION	PAGE
1. Introduction	1
2. Technique	4
3. Results and Discussions	6
4. Conclusions	7
5. References	9

LIST OF FIGURES

FIGURE		PAGE
1	Axial Residual Stress Distribution and Peak Width Distribution	14

LIST OF TABLES

TABLE		PAGE
1.	Surface Axial Residual Stresses	10
2.	Residual Stress Depth Analysis \Room Temperature Baseline Blade	11
3.	Residual Stress Depth Analysis \450°F Blade	12
4.	Residual Stress Depth Analysis \750°F Blade	13

1. INTRODUCTION

The surface of any component that undergoes mechanical loading is particularly important in influencing the fatigue life of that part. The factors that contribute to surface fatigue sensitivity are less slip restriction at the surface, the existence of single edge cracks, the surface sees large tensile gradients when the part is exposed to bending and torsion, the surface tends to be an area of multiple defects and the surface is the most sensitive region to environmental effects such as corrosion. Compressive residual stresses are utilized in the turbine engine environment to counteract regions on the surface that must withstand high tensile stresses.

These tensile regions can be created by manufacturing processes and operational loads. Typically, concentrations of tensile residual stress are introduced during part manufacturing by processes such as electro-discharge machining, electro-chemical machining, grinding, polishing and welding. In turbine engine rotors the areas of highest preload tensile stress are blade root fillets and in blade and disk dovetail fillets. These areas are also the locations of highest tensile load during operation due to the high radial stress high temperature environment and the combination of high cycle fatigue (HCF) and low cycle fatigue (LCF). In the past, this dovetail region has led to a number of component failures due to fretting fatigue. Furthermore, advanced concepts in turbomachinery design facilitates the need for tensile stress reduction. Blisks (one piece blade disk parts) are being developed to increase efficiency, but the unique blade-disk region has several design limitations that revolve around regions of high tensile stress. There are also studies looking at forward swept blades, because they may improve efficiency, but the trailing edge of these components are also limited by large tensile stress gradients. Turbine engine materials are sometimes exposed to a very aggressive corrosive environment by fuel leaks, hydraulic leaks and by operating near

coastal waters. Tensile stresses increase the corrosive rate of processes such as hydrogen embrittlement and stress corrosion cracking.

Compressive residual stresses remove the tensile residual created by manufacturing and significantly reduce the tensile load on the surface induced by operational processes. Since most cracks initiate at the surface under bending loads, a reduction in the surface tensile stress will ensure longer life under high cycle (low stress) conditions. The magnitude of the superposition of the compressive stress unto the tensile stress region is critical to the suppression of crack growth. Ideally, the superposition of compressive and tensile forces would result in a K_{max} where ΔK at the surface would be less than the threshold ΔK of the material. In this situation cracks would be arrested, but the threshold limits of most materials are below the stress gradients seen at the surface during operation. As one travels further through the depth of the component, the bending loads are decreased and usually there will lie some point just below the surface where cracks will be arrested. These factors limit compressive residual stresses to regions of high cycle fatigue and relatively low stress regions. Surface compressive stresses typically reach a magnitude of 50 percent of the parent material yield stress and penetrate to depths of less than 5 mils. In regions of low cycle fatigue (higher tensile stresses), the crack tip plastic zone tensile stress exceeds the compressive residual stress and cracks propagate.

Compressive residual stresses have certain part location limitations and they also have intrinsic limitations. They have in extreme cases caused internal defects, which are a result of tensile spikes that balance the compressive residual. The force used to create the compressive residuals can distort the edge of the component and knock it out of specifications. Finally, the residuals are prone to "relax out" after several thousand cycles and they relax out when they are exposed to temperatures above their thermomechanical limitations

(temperatures at which grain growth occurs). This study is to determine whether the compressive residual created by laser shock processing is robust enough to handle the cold section temperature (750°F) requirements of most turbine engines.

The purpose of this investigation was to determine if there was any significant stress relaxation in the laser processed areas due to elevated temperature exposure, and to determine if there was any change in the surface stresses at the transition region between the laser processed and the non-laser processed regions. Before laser shock processing can be transitioned for use in turbine engines, it must demonstrate that it can withstand the harsh environment. Three F101 first stage fan blades (material Ti -8-1-1) were laser processed for the purpose of determining the axial surface and subsurface residual stress distributions.

2. TECHNIQUE

X-ray diffraction residual stress measurements were made at the surface and at nominal depths of 1, 3, 5, 7, 10, 20, 30, and 40×10^{-3} in. Subsurface measurements were made approximately 1.37 in. from the platform and 0.25 in. from the edge on the convex side of the blades in the laser processed area. Measurements were made at the surface only in the axial direction 0.25 in. from the edge on the convex side of the baseline blade at distances of 0.50, 2.50, 3.15, 4.15, and 7.25 in. from the platform. All of the measurements were made in an axial direction.

The samples were rocked through an angular range of ± 1.0 deg. around the mean psi angles during measurement to integrate the diffracted intensity over more grains, minimizing the influence of the grain size. X-ray diffraction residual stress measurements were performed using a two-angle sine-squared-psi technique, in accordance with GE specification 4013195-991 and SAE J784a, employing the diffraction of copper K-alpha radiation from the (21.3) planes of the HCP structure of the Ti 8-1-1. The diffraction peak angular positions at each of the psi tilts employed for measurement were determined from the position of the K-alpha 1 diffraction peak separated from the superimposed K-alpha doublet assuming a Pearson VII function diffraction peak profile in the high back-reflection region.⁽¹⁾ The diffracted intensity, peak breadth, and position of the K-alpha 1 diffraction peak were determined by fitting the Pearson VII function peak profile by least squares regression after correction for the Lorentz polarization and absorption effects and for a linearly sloping background intensity.

Details of the diffractometer fixturing are outlined below:

Incident Beam Divergence: 1.0 deg.

Detector: Si(Li) set for 90% acceptance of the
copper K-alpha energy

Psi Rotation: 0 to 40 deg.

Irradiated Area: 0.20 in. x 0.20 in. for the subsurface location
0.20 in. x 0.08 in. for the surface only locations
(short axis in the direction of measurement)

The value of the x-ray elastic constant, $E/(1 + \nu)$, required to calculate the macroscopic residual stress from the strain measured normal to the (21.3) planes of Ti-6Al-4V was previously determined empirically ⁽²⁾ employing a simple rectangular beam manufactured from Ti-6Al-4V loaded in four-point bending on the diffractometer to known stress levels and measuring the resulting change in the spacing of the (21.3) planes. No attempt was made to determine the x-ray elastic constant of the Ti 8-1-1 employed in the manufacture of the laser processed blades.

Material was removed electrolytically for subsurface measurement, minimizing possible alteration of the subsurface residual stress distribution as a result of material removal. All data obtained as a function of depth were corrected for the effects of the penetration of the radiation employed for residual stress measurement into the subsurface stress gradient.⁽³⁾ The stress gradient correction applied to the last depth measured is based upon an extrapolation to greater depths, and may result in over corrections at the last depth if the stress profile has

been terminated in the presence of a steep gradient. Corrections for sectioning stress relaxation and for stress relaxation caused by layer removal⁽⁴⁾ are applied as appropriate.

For the measurements performed at the surface only during this investigation, it was not possible to correct the results for the effects of penetration of the radiation employed for residual stress measurement into the subsurface stress gradient. The magnitude of this correction can be quite significant, particularly on machined or ground surfaces, and can even change the sign of surface results.

3. RESULTS AND DISCUSSION

The axial residual stress distributions measured as functions of depth are presented in Tables II, III, and IV, and are shown graphically in Figure 1. The results obtained at the surface only are presented in Table 1. Compressive stresses are shown as negative values, tensile as positive, in units of ksi (10^3 psi) and MPa (10^6 N/m²). The results shown in each computer generated table of macroscopic residual stress data are given first as measured, then after correction for the penetration of the radiation employed for measurement into the subsurface stress gradient, and finally for stress relaxation which occurred as a result of removing layers of material by electropolishing for subsurface measurement and sectioning, as appropriate. The fully corrected data, shown in the column titled, "Relaxation," are plotted in the associated figure. For cylindrical samples from which complete shells were removed for subsurface measurement, the radial stress is calculated assuming a rotationally symmetrical residual stress distribution. The angular width of the (21.3) K-alpha 1 diffraction peak at half height is shown in the far right-hand column.

In each figure, the macroscopic residual stress distribution is plotted in the upper graph. The lower graph gives the (21.3) diffraction peak width distribution. The (21.3) diffraction peak width was calculated simultaneously with the macroscopic residual stress from the peak width in the $\psi = 0$ orientation. The (21.3) diffraction peak width is a sensitive function of the chemistry, hardness, and the degree to which the material has been cold worked. In martensitic steels, it is commonly observed that plastic deformation produced by processes such as shot peening or grinding will cause work softening, and a reduction in the peak width. In work hardening materials, the diffraction peak width increases significantly as a result of an increase in the average microstrain and the reduced crystallite size produced by cold working. The (21.3) diffraction peak width can be indicative of how the material may have been processed, and the depth to which it has been plastically deformed.

The error shown for each residual stress measurement is one standard deviation resulting from random error in the determination of the diffraction peak angular positions and in the empirically determined value of $E/(1 + \nu)$ in the $\langle 21.3 \rangle$ direction. An additional semisystematic error on the order of ± 2 ksi (± 14 MPa) may result from sample positioning and instrument alignment errors. The magnitude of this systematic error was monitored using a powdered metal zero-stress standard in accordance with ASTM specification E915, and found to be ± 0.4 ksi during the course of this investigation.

4. CONCLUSIONS

The surface residual stress measurements made on the baseline blade as a function of distance from the platform are summarized in Table 1. The surface stresses are highest at a

distance of 0.5 in. from the platform, on the order of -134 ksi, and decrease to -71 ksi at a distance of 7.25 in. from the platform. Because the surface residual stresses are highly compressive at the surface, both inside and outside of the laser processed area, it was not possible to clearly identify a transition between the laser processed and the non-laser processed areas. The uniform compressive surface is the result of prior shot peening. Therefore, a recommendation would be to use shot peening in conjunction with laser shock processing in order to ensure that the surface of the impacted component remains in compression.

The residual stress distributions measured in the laser processed areas of the three blades are plotted in Figure 1. The results show maximum compressive stresses on the surface ranging from -99 ksi to -108 ksi. The stresses decrease in compression from the surface and cross the zero-stress axis at nominal depths of 0.015 in. for the 450°F specimen and 0.020 in. for the baseline specimen and the 750°F specimen. The distributions are comparable from the surface to a nominal depth of 0.010 in. for all three specimens and after 0.010 in. for the 750°F specimen and the baseline specimen.

The stress distributions in the three blades are nearly identical. Neither of the blades exposed to elevated temperature showed any significant stress relaxation due to the thermal exposure. This was expected, since the thermal stability limit of Ti 8-1-1 is approximately 900°F.

5. REFERENCES:

- (1) P.S. Prevey, ADV. IN X-RAY ANAL., Vol. 29, 1986, pp. 103-112.
- (2) P.S. Prevey, ADV. IN X-RAY ANAL., Vol. 20, 1977, pp. 345-354.
- (3) D.P. Koistinen and R.E. Marburger, Trans. ASM, Vol. 51, 1959, p. 537.
- (4) M.G. Moore and W.P. Evans, Trans. SAE, Vol. 66, 1958, p. 340.

Table 1

SURFACE AXIAL RESIDUAL STRESSES

DISTANCE FROM PLATFORM (in.)	RESIDUAL STRESS (ksi)	PEAK WIDTH (deg.)
0.6	-133.8	1.53
1.375	-104.5	1.83
2.250	-84.8	1.63
3.15	-85.8	1.60
4.15	-78.9	1.60
7.25	-71.3	1.58

Table 2

RESIDUAL STRESS DEPTH ANALYSIS

Room Temperature Baseline Blade

	DEPTH		RESIDUAL STRESS ksi (MPa)						B
	in.	(mm)	Measured			Gradient		Relaxation	(deg)
1	0.0000	(0.0000)	-104.5 \pm 1.7	(-720 \pm 11.)	-108.2(-746.)	-108.2(-746.) 1.83
2	0.0010	(0.0254)	-92.4 \pm 1.4	(-637 \pm 10.)	-94.4(-651.)	-90.4(-623.) 1.40
3	0.0030	(0.0762)	-87.3 \pm 1.3	(-602 \pm 9.)	-87.7(-605.)	-76.6(-528.) 1.26
4	0.0052	(0.1321)	-78.8 \pm 1.3	(-543 \pm 9.)	-79.3(-547.)	-61.0(-421.) 1.22
5	0.0072	(0.1829)	-75.8 \pm 1.2	(-522 \pm 8.)	-75.8(-523.)	-51.7(-356.) 1.28
6	0.0101	(0.2565)	-78.2 \pm 1.2	(-539 \pm 9.)	-78.1(-538.)	-45.5(-314.) 1.25
7	0.0200	(0.5080)	-57.5 \pm 1.1	(-397 \pm 8.)	-57.9(-399.)	-1.6(-11.) 1.24
8	0.0293	(0.7442)	-43.6 \pm 1.0	(-301 \pm 7.)	-43.7(-302.)	24.3(167.) 1.19
9	0.0406	(1.0312)	-47.4 \pm 1.1	(-327 \pm 7.)	-46.9(-324.)	30.1(208.) 1.30

Table 3

RESIDUAL STRESS DEPTH ANALYSIS

450°F Blade

	DEPTH		RESIDUAL STRESS ksi (MPa)						B	
	in.	(mm)	Measured			Gradient		Relaxation	(deg)	
1	0.0000	(0.0000)	-98.9 _± 1.5	(-682 _± 10.)	-102.7(-708.)	-102.7(-708.)	-102.7(-708.)	1.55		
2	0.0009	(0.0229)	-88.7 _± 1.3	(-612 _± 9.)	-90.7(-626.)	-87.3(-602.)	-87.3(-602.)	1.22		
3	0.0030	(0.0762)	-86.5 _± 1.3	(-597 _± 9.)	-86.9(-599.)	-76.2(-525.)	-76.2(-525.)	1.31		
4	0.0052	(0.1321)	-77.0 _± 1.2	(-531 _± 8.)	-77.6(-535.)	-59.8(-412.)	-59.8(-412.)	1.28		
5	0.0071	(0.1803)	-72.3 _± 1.2	(-499 _± 8.)	-72.8(-502.)	-49.5(-342.)	-49.5(-342.)	1.14		
6	0.0106	(0.2692)	-65.9 _± 1.1	(-454 _± 8.)	-66.4(-458.)	-34.1(-235.)	-34.1(-235.)	1.16		
7	0.0201	(0.5105)	-24.1 _± .9	(-166 _± 6.)	-24.4(-168.)	19.9(137.)	19.9(137.)	1.05		
8	0.0303	(0.7696)	-44.0 _± 1.0	(-303 _± 7.)	-43.7(-301.)	8.1(56.)	8.1(56.)	1.19		
9	0.0396	(1.0058)	-47.4 _± 1.0	(-327 _± 7.)	-45.5(-327.)	16.5(114.)	16.5(114.)	1.19		

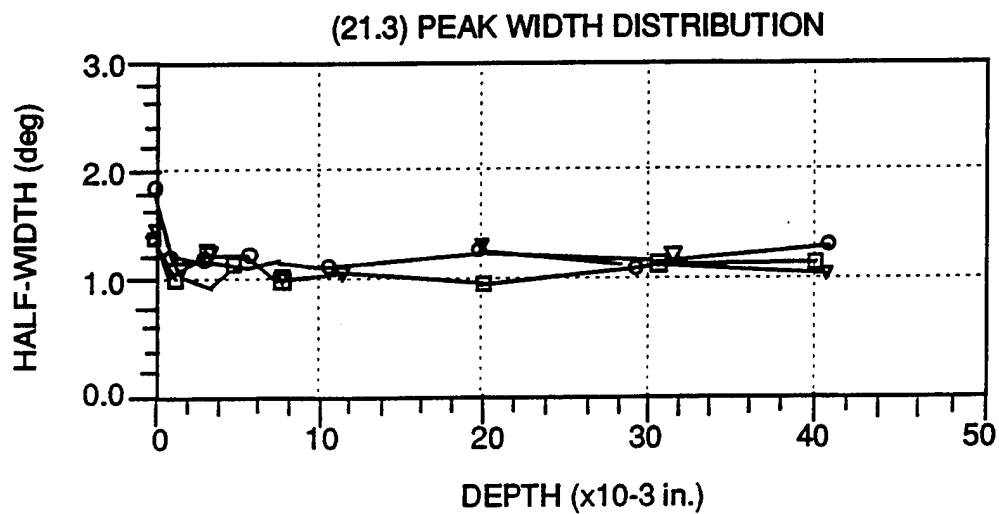
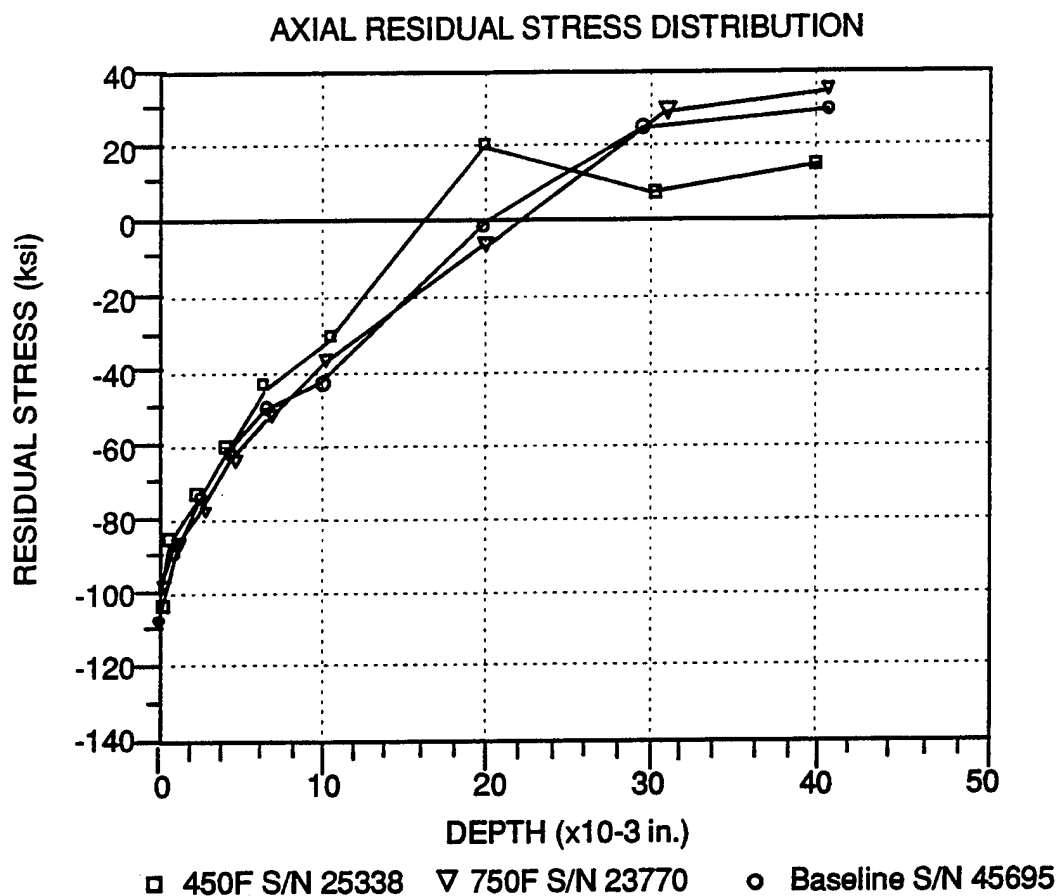
Table 4

RESIDUAL STRESS DEPTH ANALYSIS

750°F Blade

	DEPTH		RESIDUAL STRESS ksi (MPa)				B	
	in.	(mm)	Measured	Gradient	Relaxation		(deg)	
1	0.0000	(0.0000)	-96.9 ± 1.5 (-668 ± 10.)	-98.5(-679.)	-98.5(-679.)		1.53	
2	0.0011	(0.0279)	-91.5 ± 1.3 (-631 ± 9.)	-92.3(-636.)	-88.1(-607.)		1.28	
3	0.0030	(0.0762)	-91.6 ± 1.3 (-631 ± 9.)	-91.9(-633.)	-80.8(-557.)		1.12	
4	0.0053	(0.1346)	-81.8 ± 1.3 (-564 ± 9.)	-82.3(-568.)	-63.4(-437.)		1.26	
5	0.0071	(0.1803)	-75.4 ± 1.2 (-520 ± 8.)	-75.6(-521.)	-51.3(-354.)		1.14	
6	0.0100	(0.2540)	-75.9 ± 1.2 (-524 ± 8.)	-75.9(-523.)	-43.4(-299.)		1.22	
7	0.0202	(0.5131)	-64.4 ± 1.1 (-444 ± 8.)	-64.7(-446.)	-6.7(-46.)		1.26	
8	0.0308	(0.7823)	-47.1 ± 1.0 (-325 ± 7.)	-47.3(-326.)	26.2(181.)		1.23	
9	0.0406	(1.0312)	-47.5 ± 1.0 (-328 ± 7.)	-47.3(-327.)	34.0(235.)		1.14	

Figure 1



Ti-8-1-1 BLADE
Laser Processed Area